



ATM loss leads to synthetic lethality in BRCA1 BRCT mutant mice associated with exacerbated defects in homology-directed repair

Chun-Chin Chen^{a,b}, Elizabeth M. Kass^a, Wei-Feng Yen^{b,c}, Thomas Ludwig^d, Mary Ellen Moynahan^e, Jayanta Chaudhuri^c, and Maria Jasin^{a,b,1}

^aDevelopmental Biology Program, Memorial Sloan Kettering Cancer Center, New York, NY 10065; ^bBiochemistry & Structural Biology, Cell & Developmental Biology, and Molecular Biology (BCMB) Allied Program, Weill Cornell Graduate School of Medical Sciences, Cornell University, New York, NY 10065; ^cImmunology Program, Memorial Sloan Kettering Cancer Center, New York, NY 10065; ^dDepartment of Cancer Biology and Genetics, Ohio State University College of Medicine, Columbus, OH 43210; and ^eDepartment of Medicine, Memorial Sloan Kettering Cancer Center, New York, NY 10065

Contributed by Maria Jasin, June 2, 2017 (sent for review April 18, 2017; reviewed by Junjie Chen and Lee Zou)

BRCA1 is essential for homology-directed repair (HDR) of DNA double-strand breaks in part through antagonism of the nonhomologous end-joining factor 53BP1. The ATM kinase is involved in various aspects of DNA damage signaling and repair, but how ATM participates in HDR and genetically interacts with BRCA1 in this process is unclear. To investigate this question, we used the *Brcal*^{S1598F} mouse model carrying a mutation in the BRCA1 C-terminal domain of BRCA1. Whereas ATM loss leads to a mild HDR defect in adult somatic cells, we find that ATM inhibition leads to severely reduced HDR in *Brcal*^{S1598F} cells. Consistent with a critical role for ATM in HDR in this background, loss of ATM leads to synthetic lethality of *Brcal*^{S1598F} mice. Whereas both ATM and BRCA1 promote end resection, which can be regulated by 53BP1, *53bp1* deletion does not rescue the HDR defects of *Atm* mutant cells, in contrast to *Brcal* mutant cells. These results demonstrate that ATM has a role in HDR independent of the BRCA1–53BP1 antagonism and that its HDR function can become critical in certain contexts.

ATM | BRCA1 | homology-directed repair | homologous recombination | olaparib

A DNA double-strand break (DSB) is one of the most cytotoxic types of DNA damage and poses a significant threat to genome integrity. Two major DSB repair pathways exist in mammalian cells: homology-directed repair (HDR) and nonhomologous end joining (NHEJ) (1, 2). In NHEJ, DNA ends are minimally processed before rejoining. By contrast, HDR initiates with resection of DNA ends to generate single-strand DNA for RAD51-mediated strand invasion of a homologous template. HDR is considered a relatively error-free repair pathway, such that defects in HDR result in the use of more error-prone repair mechanisms that predispose cells to genome instability and tumorigenesis or cell death.

An essential HDR factor is the breast tumor suppressor BRCA1, which promotes the initial end resection step of HDR, as well as later steps (1, 3). HDR defects in BRCA1-deficient cells can be suppressed by loss of 53BP1, an NHEJ protein that impedes end resection (4–6). BRCA1 and 53BP1 operate antagonistically at different cell cycle phases: 53BP1 and interacting proteins RIF1 and PTIP counteract BRCA1 in G1 phase to limit end resection; by contrast, BRCA1 suppresses 53BP1 function in S/G2 phases to promote resection (3, 7). In addition to antagonizing 53BP1, BRCA1 binds to the resection factor CtIP and facilitates its activity, although the mechanisms merit further investigation (8–11).

ATM kinase is the master regulator of the DNA damage signaling and repair machinery in response to DSBs, and a suppressor of lymphoid and mammary tumors (12, 13). In repair, ATM is implicated in various aspects of NHEJ, e.g., in maintaining the fidelity of the joining process (14, 15). ATM-mediated phosphorylation is required for the proper functioning of 53BP1 in NHEJ (3, 7) and for the destabilization of BRCA1–PALB2 complex to prevent HDR in G1 phase (16). Conversely, ATM is also proposed to

participate in HDR (17, 18), e.g., by phosphorylating CtIP in cooperation with cyclin-dependent kinase to stimulate end resection in S/G2 phases (19–23). However, several studies have shown that ATM is not essential for HDR in some contexts, e.g., mouse embryonic stem (ES) cells (24–27). Further, unlike the severe phenotypes of mice deficient in core HDR factors such as BRCA1 (28), *Atm* nullizygous mice are viable (29, 30). Therefore, it remains an open question whether ATM plays a significant role in HDR.

In this study, we examine the genetic interactions between ATM, BRCA1, and 53BP1 in mice using a hypomorphic mutant, *Brcal*^{S1598F} (*Brcal*^{SF}), carrying a mutation in the BRCA1 C-terminal (BRCT) domain (31). We present evidence that ATM is critical for the residual HDR in *Brcal*^{SF} cells, and that loss of ATM in *Brcal*^{SF} mice leads to synthetic lethality, consistent with the embryonic lethality of mouse mutants with severe HDR defects. Interestingly, unlike in the *Brcal*^{SF} mutant, the resection and HDR defects in the *Atm* mutant cannot be rescued by *53bp1* deletion. These genetic analyses indicate that ATM has a role in HDR independent of the BRCA1–53BP1 antagonism and, although normally not essential for HDR, this role becomes critical when certain functions of BRCA1 are compromised.

Results

ATM Inhibition Reduces HDR in *Brcal*^{SF} Embryonic Stem Cells. Because BRCA1 and ATM have both been implicated in DNA end

Significance

The tumor suppressors BRCA1 and ATM have both been implicated in the early steps of homologous recombination, also termed homology-directed repair (HDR). However, how ATM genetically interacts with BRCA1 in this process is unclear. In mice carrying a breast cancer-derived mutation in the BRCA1 C-terminal (BRCT) domain, we find that ATM becomes essential for supporting the residual levels of HDR necessary to repair a DNA break. ATM-mediated HDR is not affected by the status of 53BP1, an antagonizing factor of BRCA1. ATM loss is associated with synthetic lethality of BRCT mutant mice, which provides insight into the therapeutic potential of utilizing ATM kinase inhibitors in combination with PARP-inhibitor therapy for certain BRCA1-deficient tumors.

Author contributions: C.-C.C., E.M.K., and M.J. designed research; C.-C.C., E.M.K., and W.-F.Y. performed research; C.-C.C., E.M.K., and T.L. contributed new reagents/analytic tools; C.-C.C., E.M.K., W.-F.Y., T.L., M.E.M., J.C., and M.J. analyzed data; and C.-C.C., E.M.K., and M.J. wrote the paper.

Reviewers: J.C., University of Texas MD Anderson Cancer Center; and L.Z., Massachusetts General Hospital Cancer Center.

The authors declare no conflict of interest.

¹To whom correspondence should be addressed. Email: m-jasin@ski.mskcc.org.

This article contains supporting information online at www.pnas.org/lookup/suppl/doi:10.1073/pnas.1706392114/-DCSupplemental.

resection, for the first step of HDR, we investigated the genetic interaction of the two proteins. Whereas complete loss of BRCA1 leads to cell lethality, mice expressing BRCA1 S1598F (SF) are viable; this mutation ablates the interaction of the BRCA1 BRCT domain with phosphoproteins (31) (Fig. 1A). HDR was substantially reduced in mouse *Brca1^{SF/SF}* ES cells, as demonstrated using the direct repeat (DR)-GFP reporter assay (more than fivefold) (31) (Fig. 1B). By contrast, HDR levels were not significantly reduced in the *Atm^{-/-}* cells (Fig. 1B and *SI Appendix, Fig. S1A*), as previously reported (25–27), indicating that ATM is not required for HDR in these cells. However, we observed that HDR was reduced at an earlier time point (i.e.,

24 vs. 48 h after transfection), such that *Atm^{-/-}* ES cells showed a delay in HDR, but eventually reached wild-type (WT) levels.

To examine the interaction between ATM and the BRCA1 mutant, ES cells were treated with an ATM inhibitor (ATMi) KU-55933. ATMi treatment reduced HDR in both WT and *Brca1^{SF/SF}* cells; the reduction was greater in *Brca1^{SF/SF}* cells, leading to an overall 19-fold reduction in HDR compared with DMSO-treated WT cells (Fig. 1C). These differences were not related to changes in cell cycle distribution (*SI Appendix, Fig. S1B*). Thus, ATM kinase activity supports HDR in *Brca1^{SF/SF}* cells.

We also examined the response of these ES cell lines to olaparib, a poly(ADP ribose) polymerase inhibitor (PARPi), treatment of which is synthetically lethal with HDR deficiency (32). Transient olaparib exposure had little effect on WT ES cells at the doses tested, but decreased colony formation of both mutants (Fig. 1D). Interestingly, *Atm^{-/-}* ES cells showed a similar sensitivity as *Brca1^{SF/SF}* cells, despite only a kinetic delay in HDR in the DR-GFP assay, suggesting additional repair deficiencies such as processing of DNA ends at trapped PARP complexes (33). ATM inhibition in *Brca1^{SF/SF}* cells led to extreme sensitivity of these cells to olaparib in colony formation assays (Fig. 1D and *SI Appendix, Fig. S1C*), consistent with the exacerbated HDR defect.

The mouse *Brca1^{SF}* mutation encodes a protein that corresponds to the familial breast cancer mutation S1655F, which disrupts the interaction of the BRCT domain with a number of phosphoproteins, including the resection factor CtIP (34). Previous studies have shown that phosphorylation of human CtIP at residue S327 (S326 in mouse) mediates its interaction with BRCA1 (35). CtIP phosphorylation at this residue is not essential for end resection but can stimulate the process (10).

We asked whether mouse cells expressing CtIP S326A, which is deficient in binding BRCA1 (8), recapitulate *Brca1^{SF}* mutant phenotypes and have a similar dependence on ATM for HDR. Unlike *Brca1^{SF/SF}* ES cells, *Ctip^{S326A/-}* ES cells showed no significant reduction in HDR, as reported previously (8) (*SI Appendix, Fig. S1D*), and ATMi treatment reduced HDR in *Ctip^{S326A/-}* cells to a similar extent as in *Ctip^{+/-}* cells (*SI Appendix, Fig. S1E*). Further, *Ctip^{S326A/-}* cells showed only a mild sensitivity to olaparib compared with *Brca1^{SF/SF}* cells and, whereas inhibition of ATM in the olaparib-treated *Ctip^{S326A/-}* cells reduced survival more than that in *Ctip^{+/-}* cells, it was not equivalent to the extreme hypersensitivity of the similarly treated *Brca1^{SF/SF}* cells (Fig. 1E). Thus, disruption of the interaction of CtIP with BRCA1 does not recapitulate the phenotype of *Brca1^{SF/SF}* cells, including the degree of dependence on ATM for HDR, and suggests that loss of interaction of the BRCT domain with other or additional factors is responsible for the phenotype of these cells.

***Brca1^{SF}* Mutation Is Synthetically Lethal with *Atm* Nullizyosity.** *Brca1^{Δ11/Δ11}* mice that express the exon 10–12 spliced product of BRCA1 with an intact BRCT domain die during embryogenesis (36), but loss of ATM or CHK2 rescues the embryonic lethality (37). Presumably, unrepaired DNA damage triggers a DNA damage response through ATM–CHK2 that confers a survival disadvantage to *Brca1^{Δ11/Δ11}* embryos.

Brca1^{SF/SF} mice show a less penetrant phenotype than *Brca1^{Δ11/Δ11}* mice: *Brca1^{SF/SF}* mice can be recovered, but they were observed at about half the expected Mendelian frequency at weaning (Fig. 2A). To determine whether the reduced survival of *Brca1^{SF/SF}* mice could be rescued by dampening the DNA damage response or whether the role for ATM in HDR becomes important in this context, matings were performed to generate *Atm^{-/-}Brca1^{SF/SF}* and *Chk2^{-/-}Brca1^{SF/SF}* mice. Heterozygous *Atm* deletion, as well as heterozygous and homozygous deletion of *Chk2*, partially rescued the *Brca1^{SF/SF}* mice (Fig. 2A and B), indicating that a DNA damage response reduces the survival of *Brca1^{SF/SF}* mice. However, we did not recover viable *Atm^{-/-}Brca1^{SF/SF}* double mutants, indicating that ATM is required for the survival of *Brca1^{SF/SF}* mice

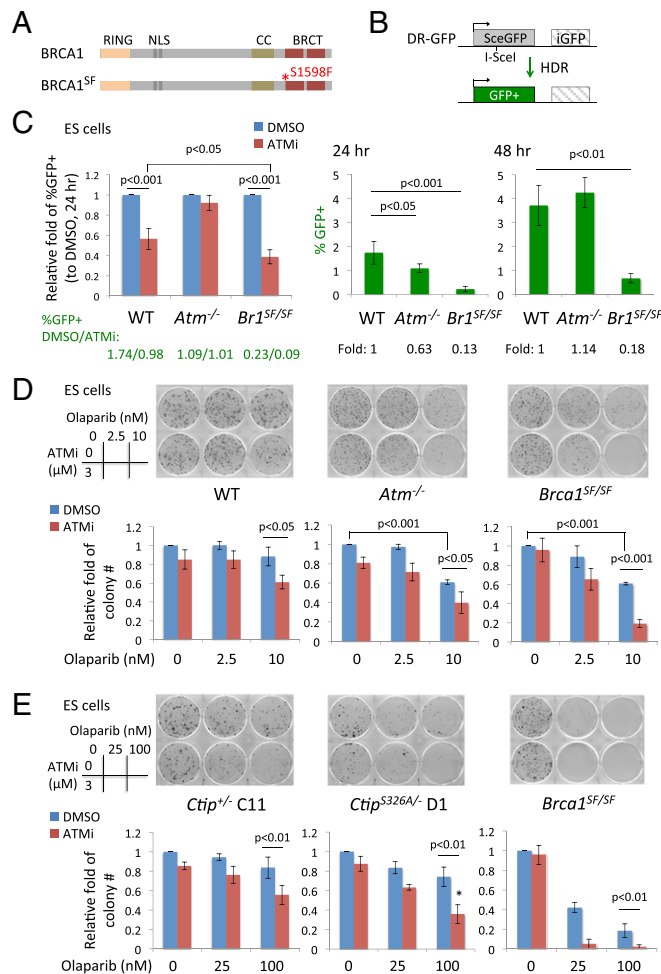


Fig. 1. ATM inhibition reduces HDR in *Brca1^{SF/SF}* ES cells. (A) Mouse BRCA1 S1598F (SF) protein has a point mutation in the BRCT domain that disrupts the interaction with phosphoproteins. (B) The DR-GFP reporter consists of two copies of mutant GFP genes. A DSB introduced by I-SceI endonuclease in *SceGFP* can be repaired by HDR using *iGFP* as a template and restore a functional *GFP+* gene. HDR is substantially reduced in *Brca1^{SF/SF}* ES cells. HDR in *Atm^{-/-}* ES cells has no significant difference from WT cells, however a ~40% reduction is seen at an earlier time point (24 h posttransfection of an I-SceI-expression vector). All error bars represent 1 SD from the mean. ($n \geq 3$). (C) ATMi (3 μ M) treatment suppresses HDR to a greater extent in *Brca1^{SF/SF}* than in WT ES cells. ($n = 5$). (D) *Brca1^{SF/SF}* ES cells show a further reduction in colony number upon the combined treatment of olaparib (2 d) and ATMi (continuous). The fold is relative to the colony number of DMSO treatment. ($n = 3$). (E) ATMi-treated *Ctip^{S326A/-}* ES cells are slightly more sensitive to olaparib compared with *Ctip^{+/-}* cells; however, the level is not comparable to the hypersensitivity in *Brca1^{SF/SF}* cells. * $P < 0.05$ vs. *Ctip^{+/-}* ($n = 4$). CC, coiled coil; NLS, nuclear localization signal.

A $Atm^{-/-}Brca1^{SF/+}$ x $Atm^{+/+}Brca1^{SF/+}$ (Total: 463) *2 dead pups found at birth

| <i>Atm</i> | +/+ | | | +/- | | | -/- | | |
|---------------------------|------|------|-------|------|-------|-------|------|------|-------|
| <i>Brca1^{SF}</i> | +/+ | SF/+ | SF/SF | +/+ | SF/+ | SF/SF | +/+ | SF/+ | SF/SF |
| Observed | 33 | 72 | 16 | 63 | 157 | 44 | 31 | 47 | *0 |
| Expected | 28.9 | 57.9 | 28.9 | 57.9 | 115.8 | 57.9 | 28.9 | 57.9 | 28.9 |

B $Chk2^{-/-}Brca1^{SF/+}$ x $Chk2^{+/+}Brca1^{SF/+}$ (Total: 183)

| <i>Chk2</i> | +/+ | | | +/- | | | -/- | | |
|---------------------------|------|------|-------|------|------|-------|------|------|-------|
| <i>Brca1^{SF}</i> | +/+ | SF/+ | SF/SF | +/+ | SF/+ | SF/SF | +/+ | SF/+ | SF/SF |
| Observed | 15 | 28 | 1 | 31 | 51 | 18 | 11 | 22 | 6 |
| Expected | 11.4 | 22.9 | 11.4 | 22.9 | 45.8 | 22.9 | 11.4 | 22.9 | 11.4 |

C $Atm^{-/-}Brca1^{SF/+53bp1^{-/-}}$ x $Atm^{+/+}Brca1^{SF/+53bp1^{-/-}}$ (Total: 483)

| <i>Brca1^{SF}</i> | <i>SF/SF</i> | | | | | | Others | | |
|---------------------------|--------------|-------|------|-------|-------|-------|--------|-------|--------|
| <i>53bp1</i> | +/+ | | +/- | | -/- | | | | |
| <i>Atm</i> | +/+ | -/- | +/+ | -/- | +/+ | -/- | +/+ | -/- | -/- |
| Observed | 5 | 8 | 0 | 11 | 33 | 3 | 7 | 18 | 5 |
| Expected | 7.55 | 15.09 | 7.55 | 15.09 | 30.19 | 15.09 | 7.55 | 15.09 | 7.55 |
| | | | | | | | | | 362.25 |

Fig. 2. The $Brca1^{SF}$ hypomorphic allele shows synthetic lethality with Atm nullizygosity. (A) Atm heterozygosity rescues the sub-Mendelian ratio of $Brca1^{SF/SF}$ mice. However, no live $Atm^{-/-}Brca1^{SF/SF}$ double mutant mice are recovered at weaning. (B) Heterozygous and homozygous deletion of $Chk2$ partially rescue the sub-Mendelian ratio of $Brca1^{SF/SF}$ mice. (C) Heterozygous and homozygous deletions of $53bp1$ rescue the viability of $Atm^{-/-}Brca1^{SF/SF}$ double mutant mice.

(Fig. 24). These results suggest that the lethality associated with complete loss of ATM is due to another function of ATM such as in DNA repair, specifically HDR.

To approximate at what stage $Atm^{-/-}Brca1^{SF/SF}$ mice die, timed matings were set up to harvest embryos. $Atm^{-/-}Brca1^{SF/SF}$ embryos were underrepresented at midembryogenesis, although at both embryonic days E9.5 (SI Appendix, Fig. S2A) and E13.5 (SI Appendix, Fig. S2B) one double mutant was recovered; both embryos appeared smaller than their single mutant littermates. Mouse embryonic fibroblasts (MEFs) derived from the E13.5 embryo failed to proliferate in culture. Overall, our results indicate that Atm nullizygous mutation leads to a synthetic, embryonic lethality in the context of the $Brca1^{SF}$ missense mutation, in contrast to the rescue of viability observed with the $Brca1^{\Delta11}$ allele. The difference between the two $Brca1$ alleles may relate to the BRCT domain, which is intact in the protein expressed from the $Brca1^{\Delta11}$ allele (38).

HDR in $Brca1^{SF}$ Primary Mouse Fibroblasts Is Further Reduced by ATM Inhibition. To investigate the mechanism of synthetic lethality, we examined HDR in primary fibroblasts using mice containing an integrated DR-GFP reporter and a doxycycline (Dox)-inducible I-SceI endonuclease (27, 39). Primary ear fibroblasts from the $Brca1^{SF/SF}$ and $Atm^{-/-}$ mice showed 3- and 2-fold reductions in HDR, respectively (Fig. 3A and B), whereas ATM inhibition of WT cells reduced HDR by 1.6-fold (Fig. 3C). To take into account animal variation in I-SceI expression, the percentage of GFP⁺ cells was normalized to total DSB repair events (SI Appendix, Fig. S3A), which confirmed the fold reductions in HDR (SI Appendix, Fig. S3B and C). Unlike the delay of HDR seen in $Atm^{-/-}$ ES cells, a similar reduction in HDR in $Atm^{-/-}$ compared with control ear fibroblasts was observed at all time points following DSB induction (SI Appendix, Fig. S3D). Other somatic cell types from $Atm^{-/-}$ mice, i.e., splenic B cells and mammary epithelial cells, showed similarly impaired HDR (SI Appendix, Fig. S3E and F), as did a distinct Atm mutant (30) (SI Appendix, Fig. S3G). Thus, loss of ATM causes a defect in HDR in mouse primary adult somatic cells, as measured by the DR-GFP reporter assay, although not to the same extent as with the hypomorphic $Brca1^{SF}$ allele (SI Appendix, Fig. S3B and H). $Brca1^{SF}$ heterozygosity did not significantly affect HDR when

normalized in either fibroblasts or mammary cells (SI Appendix, Fig. S3B and H).

Although ATM deficiency by itself caused only a mild HDR defect, ATM inhibition in $Brca1^{SF/SF}$ ear fibroblasts greatly exacerbated their HDR defect, such that the overall reduction of HDR relative to DMSO-treated WT cells was 14-fold (Fig. 3C). The large HDR reduction in ATMi-treated $Brca1^{SF/SF}$ cells was not related to changes in cell cycle distribution (SI Appendix, Fig. S3I). Treatment of a CHK2 inhibitor slightly reduced HDR in the $Brca1^{SF/SF}$ ear fibroblasts, but the extent was not significantly different from that in WT or $Atm^{-/-}$ cells (SI Appendix, Fig. S3J),

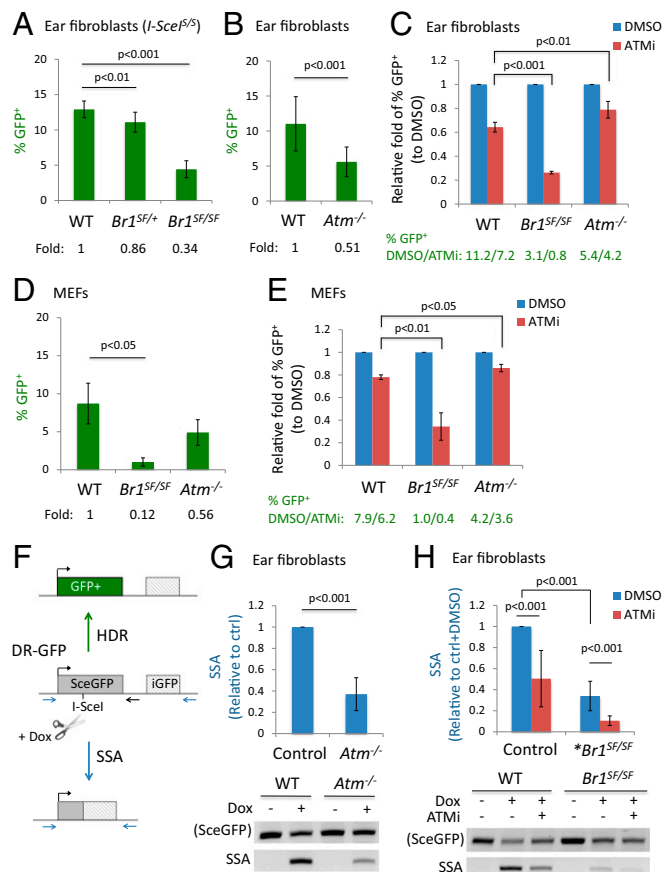


Fig. 3. ATM inhibition exacerbates HDR and SSA defects in $Brca1^{SF/SF}$ primary cells. (A) Primary ear fibroblasts from $Brca1^{SF/SF}$ mice have an ~3-fold reduction in HDR compared with WT cells. $I-SceI^{SF/SF}$: these mice are homozygous for the $TRE-I-SceI$ allele when indicated ($n \geq 9$). (B) Primary ear fibroblasts from $Atm^{-/-}$ mice have a 2-fold reduction in HDR ($n \geq 10$). (C) ATMi treatment reduces HDR in $Brca1^{SF/SF}$ ear fibroblasts to a greater extent than in WT cells ($n \geq 3$). (D) HDR is ~8-fold lower in $Brca1^{SF/SF}$ than in WT MEFs, whereas the reduction is only ~40% in $Atm^{-/-}$ MEFs. (E) ATMi treatment reduces HDR in $Brca1^{SF/SF}$ MEFs to a greater extent than in WT MEFs. (F) The inducible I-SceI/DR-GFP system consists of the DR-GFP reporter, a CMV-rtTA transactivator, and a doxycycline (Dox)-inducible I-SceI transgene. I-SceI is induced by Dox treatment and introduces a DSB in the DR-GFP reporter that if repaired by HDR, restores GFP expression. The DSB can also be repaired via SSA if resection exposes complementary strands in both $SceGFP$ and $iGFP$, which then anneal to give rise to a shortened reporter product. SSA events are detected using a specific primer set (blue) and the intensity is normalized to the structurally intact reporter using primers flanking $SceGFP$ (blue forward, black reverse). (G) The relative levels of SSA are reduced by ~2.5-fold in $Atm^{-/-}$ ear fibroblasts compared with control cells (WT or $Atm^{+/+}$). The SSA product is observed only when I-SceI is induced. Relative fold is calculated between mutant and control cells on the same gel ($n = 7$). (H) Relative levels of SSA in $Brca1^{SF/SF}$ ear fibroblasts are ~3-fold lower than in control cells, and ATMi treatment further reduces SSA in $Brca1^{SF/SF}$ cells. * $Brca1^{SF/SF}$, $Atm^{+/+}$ or $Atm^{-/-}$ ($n = 8$). All error bars represent 1 SD from the mean.

consistent with the notion that the reliance on ATM in the *Brca1^{SF}* mutant is related to its role in DNA repair.

We performed a similar analysis in MEFs. In untreated *Brca1^{SF/SF}* MEFs, the reduction in HDR was larger than in ear fibroblasts, but was similar to ES cells (~8-fold; Fig. 3D and SI Appendix, Fig. S3K), suggesting that BRCA1 has a more pronounced role in HDR in embryonic cells than adult cells. Conversely, HDR was reduced to a somewhat lesser extent in *Atm^{-/-}* MEFs and ATMi-treated WT MEFs (Fig. 3D and E), indicating a less critical role for ATM in embryonic cells. However, as with the ear fibroblasts, the HDR defect in *Brca1^{SF/SF}* MEFs was further exacerbated by ATMi treatment, such that the overall reduction in HDR was 20-fold compared with WT cells (Fig. 3E). Overall, these results demonstrate that ATM is critical for much of the residual HDR in the *Brca1^{SF/SF}* cells, potentially accounting for the synthetic lethality observed in double mutant mice.

ATM Kinase Inhibition Further Reduces SSA in *Brca1^{SF}* Mutant Cells. Evidence suggests that both BRCA1 and ATM promote DNA end resection (6, 20, 40). End resection is a common step for HDR and another homology-based DSB repair pathway, single-strand annealing (SSA), in which complementary single strands generated by resection at sequence repeats anneal, resulting in a deletion of the sequence between the repeats; thus, a defect in end resection compromises both pathways (40). By contrast, defects in downstream steps of HDR such as RAD51 filament formation increase SSA. Using a PCR-based assay with the DR-GFP reporter to quantify SSA (41) (Fig. 3F), we found that loss or inhibition of ATM reduced SSA by 2- to 2.5-fold in ear fibroblasts (Fig. 3G and H), as reported previously for mouse ES cells (42). The decreased levels of SSA are comparable to our HDR results and are consistent with a role for ATM in the end resection steps of DSB repair.

As with HDR, *Brca1^{SF/SF}* cells showed a threefold reduction in SSA (Fig. 3H), similar to cells carrying the cognate human BRCA1 mutation (43). Notably, ATM inhibition further decreased SSA in *Brca1^{SF/SF}* cells for an overall 10-fold reduction compared with WT cells, indicating that both end resection-dependent DSB repair pathways, HDR and SSA, rely heavily on ATM in *Brca1^{SF}* mutant cells.

53bp1 Deletion Does Not Restore HDR in ATM-Deficient Cells. The NHEJ protein 53BP1 suppresses DNA end resection, such that loss of 53BP1 significantly restores HDR in BRCA1-deficient cells (5, 6). Thus, we hypothesized that loss of 53BP1 would rescue the survival of *Atm-Brca1^{SF}* double mutant animals. As predicted, viable *Atm^{-/-}Brca1^{SF/SF}53bp1^{-/-}* mice were recovered (Fig. 2C). Interestingly, *53bp1* heterozygosity also led to a rescue of *Atm^{-/-}Brca1^{SF/SF}* animals, although partial. In *Brca1^{SF/SF}* fibroblasts and mammary cells, homozygous deletion of *53bp1* fully rescued the HDR defect (Fig. 4A and SI Appendix, Fig. S4A and B), indicating that the functions of BRCT domain are involved in counteracting 53BP1 (44–46). Interestingly, in both cell types, heterozygosity for the *53bp1* mutation also led to a moderate increase in HDR (~50%) (Fig. 4A and SI Appendix, Fig. S4A and C). Thus, even partial loss of 53BP1 protein increases HDR in the *Brca1^{SF}* mutant setting.

We investigated whether *53bp1* mutation would also rescue HDR defects in *Atm* mutant cells as it does in *Brca1* mutant cells. Importantly, *Atm^{-/-}53bp1^{-/-}* ear fibroblasts showed the same approximately twofold decrease in HDR as *Atm^{-/-}* cells (Fig. 4B and SI Appendix, Fig. S4D). The lack of rescue of the HDR defect in *Atm* mutant cells by *53bp1* loss indicates that ATM operates separately from the BRCA1–53BP1 antagonism in HDR. Consistent with this interpretation, HDR was approximately twofold lower in *Atm^{-/-}Brca1^{SF/SF}53bp1^{-/-}* ear fibroblasts compared with *Brca1^{SF/SF}53bp1^{-/-}* cells (Fig. 4C and SI Appendix, Fig. S4E), indicating that *53bp1* loss specifically rescues the HDR defect caused by the *Brca1^{SF}* mutation but not that of the *Atm* mutation.

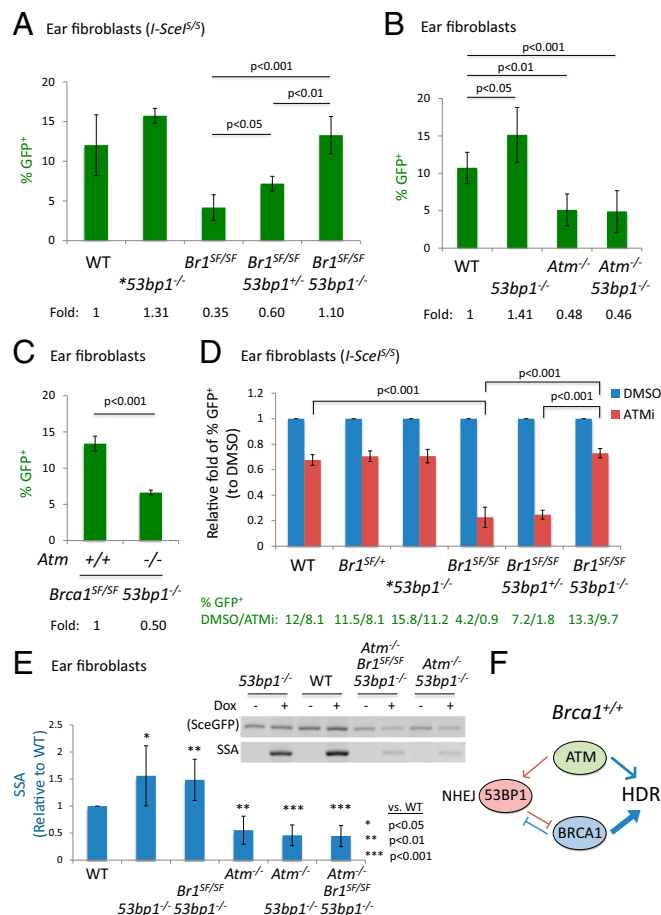


Fig. 4. ATM promotes HDR independently of the BRCA1–53BP1 antagonism. (A) HDR in *Brca1^{SF/SF}* ear fibroblasts is significantly increased by heterozygous or homozygous deletion of *53bp1*. **53bp1^{-/-}*: *Brca1^{+/+}* or *Brca1^{SF/+}* ($n \geq 3$ except $n = 2$ for *53bp1^{-/-}*). (B) Deletion of *53bp1* does not restore the HDR defect in *Atm^{-/-}* ear fibroblasts ($n \geq 4$). (C) Loss of *Atm* in *Brca1^{SF/SF}53bp1^{-/-}* ear fibroblasts reduces HDR by twofold ($n = 2$ for triple mutant). (D) ATMi treatment reduces HDR in *Brca1^{SF/SF}53bp1^{-/-}* ear fibroblasts to a similar extent as in WT or *53bp1^{-/-}* cells ($n \geq 3$ except $n = 2$ for *53bp1^{-/-}*). (E) The levels of SSA in both *Atm^{-/-}53bp1^{-/-}* and *Atm^{-/-}Brca1^{SF/SF}53bp1^{-/-}* ear fibroblasts show the similar twofold reductions as in *Atm^{-/-}* cells ($n = 4$ for *Atm^{-/-}53bp1^{-/-}* and $n = 2$ for triple mutant). (F) In *Brca1^{+/+}* cells, ATM has a minor role in HDR that operates independently of the BRCA1–53BP1 antagonism. However, ATM becomes essential for supporting the residual HDR in *Brca1^{SF/SF}* cells and the viability of *Brca1^{SF/SF}* mutant mice. All error bars represent 1 SD from the mean.

We also analyzed HDR in *Brca1^{SF/SF}53bp1^{-/-}* ear fibroblasts treated with the ATMi. HDR was significantly restored in *Brca1^{SF/SF}53bp1^{-/-}* cells compared with *Brca1^{SF/SF}* cells, but treatment of ATMi still reduced it by ~30%, similar to the fold reduction in WT cells (Fig. 4D). HDR in *53bp1^{-/-}* cells was similarly reduced by the ATMi (SI Appendix, Fig. S4F). Thus, 53BP1 loss does not rescue the HDR defect caused by either ATM loss or inhibition.

Although sensitive to ATM inhibition, the level of HDR in the *Brca1^{SF/SF}53bp1^{+/-}* cells was still higher than in the *Brca1^{SF/SF}* cells (% GFP+ 1.8 vs. 0.9, Fig. 4D), indicating that *53bp1* heterozygosity is effective in partially restoring HDR in the presence of the ATMi. Thus, it seems plausible that HDR in *Atm^{-/-}Brca1^{SF/SF}53bp1^{+/-}* mice may be restored above a threshold level that permits their survival.

ATM Supports HDR and SSA Independently of the BRCA1–53BP1 Antagonism. To further examine the interaction of the *Atm*, *Brca1^{SF}*, and *53bp1* mutations in HDR, we examined RAD51 foci

in primary ear fibroblasts (SI Appendix, Fig. S4 G and H). As seen previously in other cell types, both *Atm*^{-/-} and *Brcal*^{SF/SF} fibroblasts showed a significant decrease compared with WT in the percentage of cells positive for RAD51 foci following ionizing radiation (25% and 40% reduction, respectively) (17, 18, 20, 31), whereas *53bp1*^{-/-} cells showed a small increase (12%). In *Brcal*^{SF/SF}*53bp1*^{-/-} cells, RAD51 focus formation was significantly rescued compared with *Brcal*^{SF/SF} cells, approaching that of WT cells (SI Appendix, Fig. S4G, a, c, and f).

Consistent with the lack of rescue of HDR by 53BP1 loss (Fig. 4B), the number of RAD51 foci-positive *Atm*^{-/-}*53bp1*^{-/-} cells remained lower than WT cells (SI Appendix, Fig. S4G, a and e). Interestingly, however, a small increase was noted for the *Atm*^{-/-}*53bp1*^{-/-} compared with *Atm*^{-/-} cells, although this increase did not reach statistical significance (SI Appendix, Fig. S4G, b and e). It is possible that more recombination complexes are able to form with loss of 53BP1, which are not proficient at HDR (47); alternatively, more foci may become visible due to increased resection lengths. The *Atm*^{-/-}*Brcal*^{SF/SF}*53bp1*^{-/-} triple mutant also demonstrated reduced RAD51 foci-positive cells compared with *Brcal*^{SF/SF}*53bp1*^{-/-} (SI Appendix, Fig. S4G, f and h), further supporting a role for ATM in generating end-resected intermediates for RAD51 filament formation in cells with compromised BRCA1 and 53BP1 function.

These results suggest that ATM functions in HDR independently of 53BP1 and BRCA1 and that SSA in ATM-deficient cells would also not be fully restored by 53BP1 loss. Whereas *53bp1*^{-/-} cells had an ~1.5-fold increase in SSA, *Atm*^{-/-}*53bp1*^{-/-} cells showed the same ~2-fold reduction as *Atm*^{-/-} cells (Fig. 4E). Similarly, whereas SSA was restored in *Brcal*^{SF/SF}*53bp1*^{-/-} cells, it was reduced by ~2-fold in triple mutant cells (*Atm*^{-/-}*Brcal*^{SF/SF}*53bp1*^{-/-}, Fig. 4E) and in ATM-treated double mutant cells (SI Appendix, Fig. S4J). These results are consistent with a role for ATM in promoting resection-dependent repair independently of the BRCA1–53BP1 antagonism.

Discussion

The epistatic relationship of BRCA1 and ATM in HDR is not well understood in mice, in part because *Brcal* nullizygosity leads to early embryonic lethality (28). However, the viability of the hypomorphic *Brcal*^{SF} allele with a missense mutation in the BRCT domain (31) has allowed us to uncover synthetic lethality upon *Atm* loss. The findings support a critical role for ATM in maintaining a threshold level of HDR necessary for viability in the context of a breast cancer-associated *Brcal* mutation.

Inhibition of ATM activity in *Brcal*^{SF/SF} cells reduces HDR by up to 20-fold relative to WT cells. As HDR proficiency is essential for proliferation during mouse development (1), the contribution of ATM to HDR in *Brcal*^{SF/SF} mice provides a mechanism for the compromised viability of *Atm*–*Brcal*^{SF} double mutant mice. Previous studies have demonstrated synthetic lethality of *Atm* mutant mice with deficiency of other DNA damage response factors such as *H2ax* (48). However, the mechanisms of synthetic lethality appear to differ from what we report here. For example, *Atm*–*H2ax* double mutant cells do not show a further reduction in HDR compared with *H2ax* single mutant cells (26).

Whereas some studies have observed a role for ATM in HDR (17, 18), other studies have not (24–27). Using a highly efficient reporter system (39), we present evidence that primary somatic cells of multiple tissue types from *Atm* mutant mice have an approximately twofold reduction in HDR following an I-SceI-induced DSB. In contrast to somatic cells, our results show that ATM loss in ES cells causes only a transient delay in HDR. The lack of a defect at later time points in ES cells is consistent with findings from other groups (25, 26). Given that mouse ES cells have unique properties in DNA repair compared with more differentiated cell types (ref. 49 and references therein), it is possible that these cells have a reduced dependence on ATM by using alternative mechanisms to initiate HDR (50, 51) or simply a greater reliance on BRCA1.

Although reduced HDR in *Atm*^{-/-} cells could be associated with a role for ATM in later steps of recombination (47, 52), the shared defects in both HDR and SSA together with the reduced RPA focus formation others observe (19, 20) argue that ATM loss impacts early steps of recombination, such as regulating the end-resection machinery or the removal of Ku from DNA ends (53). ATM phosphorylates a network of end resection factors, e.g., CtIP, MRE11, and EXO1, to initiate and also modulate the extent of single-strand DNA generation (21–23, 54–56). HDR defects in *Atm* mutant cells have also been related to indirect aspects of ATM activity in chromatin relaxation (22, 57). A role for ATM in promoting end resection in HDR during S/G2 may seem contradictory, considering that ATM also functions in NHEJ: In G1 cells, ATM both supports 53BP1 function (3, 7) and inhibits end resection through phosphorylation of H2AX to promote NHEJ (58). Removing either 53BP1 or H2AX allows ATM-dependent resection to be observed (58–61), although G1 phase resection is not expected to be productive for HDR, given other restrictive mechanisms (16). Importantly, although not usually essential in wild-type cells, our results indicate that ATM becomes crucial for supporting the residual end resection and HDR in *Brcal*^{SF} hypomorphic cells, which is likely critical for the survival of *Brcal*^{SF} mice.

Our genetic epistasis indicates that the HDR and SSA defects in *Atm*^{-/-} primary cells cannot be rescued by *53bp1* deletion, distinguishing the function of ATM from the 53BP1-mediated suppression of BRCA1 and HDR. Further, whereas *53bp1* loss can restore HDR and SSA in *Brcal*^{SF/SF} cells, as with other *Brcal* mutant alleles, ATM deficiency in *Brcal*^{SF/SF}*53bp1*^{-/-} cells reduces both types of DSB repair to a similar extent as in WT or *53bp1*^{-/-} cells. Therefore, our findings support the notion that ATM has a direct function in promoting end resection independently of the BRCA1–53BP1 mutual antagonism (Fig. 4F). We do not rule out the possibility that the BRCA1^{SF} protein, which maintains ATM-phosphorylation sites (62), requires ATM phosphorylation to sustain its hypomorphic function in HDR, in which case ATM may not be an entirely independent player but may have cross-talk with BRCA1.

A number of mutations in the BRCT domain of BRCA1 have been associated with breast cancer (<https://research.nhgri.nih.gov/projects/bic/>), including S1655F equivalent to the mouse S1598F mutation. It remains to be seen how tumors carrying these mutations respond to DNA damaging agents upon ATM loss of function. The down-regulation of resection suppressors such as 53BP1 has been identified as a mechanism for the acquired resistance to PARP inhibition in BRCA1-deficient mammary tumors (63–66). Given that ATM still plays a role in HDR in these resistant cells, we envision that inhibition of ATM kinase activity may have therapeutic potential for certain types of BRCA1-deficient cancers with acquired resistance to PARP inhibitor therapy.

Materials and Methods

Mouse Care. The care and use of mice were performed with the approval of the Memorial Sloan Kettering Cancer Center (MSKCC) Institutional Animal Care and Use Committee in accordance with institutional guidelines.

HDR and Sensitivity Assays. For HDR assays in primary cells, cells at passage 1 were treated with 1 μg/mL Dox to induce I-SceI. For ATM inhibition, KU-55933 (Calbiochem) was added together with Dox and replenished at 24 h. The % GFP⁺ cells was analyzed after 48 h by flow cytometry. SSA analysis was performed as described (41). ES cells were electroporated with an I-SceI expression vector and analyzed after 24 or 48 h by flow cytometry. For drug sensitivity assays, cells were pretreated with 3 μM ATMi or DMSO for 2 h, then treated with PARPi olaparib (synthesized in the MSKCC Organic Chemistry Core Facility) in combination with ATMi or DMSO for 2 d, and then treated with ATMi or DMSO alone for another 3–4 d.

Statistical Analysis. Statistical comparisons were calculated using Student's t test.

See also SI Appendix and Dataset S1.

ACKNOWLEDGMENTS. We thank members of the M.J. laboratory for helpful discussions. This work was supported by NIH Grants K99 CA184122 (to E.M.K.); P01 CA094060 (to M.E.M. and M.J.); R01 AI072194, R01 AI124186, and U54 CA137788 (to J.C.); and R01 CA185660 and R35 GM118175 (to M.J.). This work was also supported by Stand Up To Cancer–Ovarian Cancer Research

Fund–Ovarian Cancer National Alliance–National Ovarian Cancer Coalition Dream Team Translational Research Grant SU2C-AACRDT16-15; MSKCC Support Grant/Core Grant P30 CA008748; and the Geoffrey Beene Cancer Center (J.C.), the Functional Genomics Institute (J.C.), and the Ludwig Center at MSKCC (M.J. and J.C.).

- Moynahan ME, Jasin M (2010) Mitotic homologous recombination maintains genomic stability and suppresses tumorigenesis. *Nat Rev Mol Cell Biol* 11:196–207.
- Chapman JR, Taylor MR, Boulton SJ (2012) Playing the end game: DNA double-strand break repair pathway choice. *Mol Cell* 47:497–510.
- Panier S, Boulton SJ (2014) Double-strand break repair: 53BP1 comes into focus. *Nat Rev Mol Cell Biol* 15:7–18.
- Cao L, et al. (2009) A selective requirement for 53BP1 in the biological response to genomic instability induced by Brca1 deficiency. *Mol Cell* 35:534–541.
- Bouwman P, et al. (2010) 53BP1 loss rescues BRCA1 deficiency and is associated with triple-negative and BRCA-mutated breast cancers. *Nat Struct Mol Biol* 17:688–695.
- Bunting SF, et al. (2010) 53BP1 inhibits homologous recombination in Brca1-deficient cells by blocking resection of DNA breaks. *Cell* 141:243–254.
- Zimmermann M, de Lange T (2014) 53BP1: Pro choice in DNA repair. *Trends Cell Biol* 24:108–117.
- Reczek CR, Szabolcs M, Stark JM, Ludwig T, Baer R (2013) The interaction between CtIP and BRCA1 is not essential for resection-mediated DNA repair or tumor suppression. *J Cell Biol* 201:693–707.
- Polato F, et al. (2014) CtIP-mediated resection is essential for viability and can operate independently of BRCA1. *J Exp Med* 211:1027–1036.
- Cruz-García A, López-Saavedra A, Huertas P (2014) BRCA1 accelerates CtIP-mediated DNA-end resection. *Cell Reports* 9:451–459.
- Yun MH, Hiom K (2009) CtIP-BRCA1 modulates the choice of DNA double-strand break repair pathway throughout the cell cycle. *Nature* 459:460–463.
- Shiloh Y, Ziv Y (2013) The ATM protein kinase: Regulating the cellular response to genotoxic stress, and more. *Nat Rev Mol Cell Biol* 14:197–210.
- Reiman A, et al. (2011) Lymphoid tumours and breast cancer in ataxia telangiectasia; Substantial protective effect of residual ATM kinase activity against childhood tumours. *Br J Cancer* 105:586–591.
- Bennardo N, Stark JM (2010) ATM limits incorrect end utilization during non-homologous end joining of multiple chromosome breaks. *PLoS Genet* 6:e1001194.
- Bredemeyer AL, et al. (2006) ATM stabilizes DNA double-strand-break complexes during V(D)J recombination. *Nature* 442:466–470.
- Orthwein A, et al. (2015) A mechanism for the suppression of homologous recombination in G1 cells. *Nature* 528:422–426.
- Morrison C, et al. (2000) The controlling role of ATM in homologous recombinational repair of DNA damage. *EMBO J* 19:463–471.
- Beucher A, et al. (2009) ATM and Artemis promote homologous recombination of radiation-induced DNA double-strand breaks in G2. *EMBO J* 28:3413–3427.
- Myers JS, Cortez D (2006) Rapid activation of ATR by ionizing radiation requires ATM and Mre11. *J Biol Chem* 281:9346–9350.
- Jazayeri A, et al. (2006) ATM- and cell cycle-dependent regulation of ATR in response to DNA double-strand breaks. *Nat Cell Biol* 8:37–45.
- You Z, et al. (2009) CtIP links DNA double-strand break sensing to resection. *Mol Cell* 36:954–969.
- Shibata A, et al. (2011) Factors determining DNA double-strand break repair pathway choice in G2 phase. *EMBO J* 30:1079–1092.
- Wang H, et al. (2013) The interaction of CtIP and Nbs1 connects CDK and ATM to regulate HR-mediated double-strand break repair. *PLoS Genet* 9:e1003277.
- White JS, Choi S, Bakkenist CJ (2010) Transient ATM kinase inhibition disrupts DNA damage-induced sister chromatid exchange. *Sci Signal* 3:ra44.
- Yamamoto K, et al. (2016) Kinase-dead ATM protein is highly oncogenic and can be preferentially targeted by Topo-isomerase I inhibitors. *eLife* 5:5.
- Rass E, Chandramouly G, Zha S, Alt FW, Xie A (2013) Ataxia telangiectasia mutated (ATM) is dispensable for endonuclease I-SceI-induced homologous recombination in mouse embryonic stem cells. *J Biol Chem* 288:7086–7095.
- Kass EM, et al. (2013) Double-strand break repair by homologous recombination in primary mouse somatic cells requires BRCA1 but not the ATM kinase. *Proc Natl Acad Sci USA* 110:5564–5569.
- Evers B, Jonkers J (2006) Mouse models of BRCA1 and BRCA2 deficiency: Past lessons, current understanding and future prospects. *Oncogene* 25:5885–5897.
- Xu Y, Baltimore D (1996) Dual roles of ATM in the cellular response to radiation and in cell growth control. *Genes Dev* 10:2401–2410.
- Barlow C, et al. (1996) Atm-deficient mice: A paradigm of ataxia telangiectasia. *Cell* 86:159–171.
- Shakya R, et al. (2011) BRCA1 tumor suppression depends on BRCT phosphoprotein binding, but not its E3 ligase activity. *Science* 334:525–528.
- Helleday T (2011) The underlying mechanism for the PARP and BRCA synthetic lethality: Clearing up the misunderstandings. *Mol Oncol* 5:387–393.
- Murai J, et al. (2012) Trapping of PARP1 and PARP2 by clinical PARP inhibitors. *Cancer Res* 72:5588–5599.
- Wu Q, Jubb H, Blundell TL (2015) Phosphopeptide interactions with BRCA1 BRCT domains: More than just a motif. *Prog Biophys Mol Biol* 117:143–148.
- Yu X, Chen J (2004) DNA damage-induced cell cycle checkpoint control requires CtIP, a phosphorylation-dependent binding partner of BRCA1 C-terminal domains. *Mol Cell Biol* 24:9478–9486.
- Xu X, et al. (2001) Genetic interactions between tumor suppressors Brca1 and p53 in apoptosis, cell cycle and tumorigenesis. *Nat Genet* 28:266–271.
- Cao L, et al. (2006) ATM-Chk2-p53 activation prevents tumorigenesis at an expense of organ homeostasis upon Brca1 deficiency. *EMBO J* 25:2167–2177.
- Huber LJ, et al. (2001) Impaired DNA damage response in cells expressing an exon 11-deleted murine Brca1 variant that localizes to nuclear foci. *Mol Cell Biol* 21:4005–4015.
- Kass EM, Lim PX, Helgadottir HR, Moynahan ME, Jasin M (2016) Robust homology-directed repair within mouse mammary tissue is not specifically affected by Brca2 mutation. *Nat Commun* 7:13241.
- Stark JM, Pierce AJ, Oh J, Pastink A, Jasin M (2004) Genetic steps of mammalian homologous repair with distinct mutagenic consequences. *Mol Cell Biol* 24:9305–9316.
- Nakanishi K, et al. (2005) Human Fanconi anemia monoubiquitination pathway promotes homologous DNA repair. *Proc Natl Acad Sci USA* 102:1110–1115.
- Gunn A, Bennardo N, Cheng A, Stark JM (2011) Correct end use during end joining of multiple chromosomal double strand breaks is influenced by repair protein RAD50, DNA-dependent protein kinase DNA-PKcs, and transcription context. *J Biol Chem* 286:42470–42482.
- Anantha RW, et al. (2017) Functional and mutational landscapes of BRCA1 for homology-directed repair and therapy resistance. *eLife* 6:6.
- Feng L, et al. (2015) Cell cycle-dependent inhibition of 53BP1 signaling by BRCA1. *Cell Discov* 1:15019.
- Escribano-Díaz C, et al. (2013) A cell cycle-dependent regulatory circuit composed of 53BP1-RIF1 and BRCA1-CtIP controls DNA repair pathway choice. *Mol Cell* 49:872–883.
- Kakarougkas A, et al. (2013) Co-operation of BRCA1 and POH1 relieves the barriers posed by 53BP1 and RAP80 to resection. *Nucleic Acids Res* 41:10298–10311.
- Bakr A, et al. (2015) Involvement of ATM in homologous recombination after end resection and RAD51 nucleofilament formation. *Nucleic Acids Res* 43:3154–3166.
- Zha S, Sekiguchi J, Brush JW, Bassing CH, Alt FW (2008) Complementary functions of ATM and H2AX in development and suppression of genomic instability. *Proc Natl Acad Sci USA* 105:9302–9306.
- Ahuja AK, et al. (2016) A short G1 phase imposes constitutive replication stress and fork remodelling in mouse embryonic stem cells. *Nat Commun* 7:10660.
- Duursma AM, Driscoll R, Elias JE, Cimprich KA (2013) A role for the MRN complex in ATR activation via TOPBP1 recruitment. *Mol Cell* 50:116–122.
- Peterson SE, et al. (2013) Activation of DSB processing requires phosphorylation of CtIP by ATR. *Mol Cell* 49:657–667.
- Ahlskog JK, Larsen BD, Achanta K, Sørensen CS (2016) ATM/ATR-mediated phosphorylation of PALB2 promotes RAD51 function. *EMBO Rep* 17:671–681.
- Chanut P, Britton S, Coates J, Jackson SP, Calsou P (2016) Coordinated nuclease activities counteract Ku at single-ended DNA double-strand breaks. *Nat Commun* 7:12889.
- Kijas AW, et al. (2015) ATM-dependent phosphorylation of MRE11 controls extent of resection during homology directed repair by signalling through Exonuclease 1. *Nucleic Acids Res* 43:8352–8367.
- Bolderson E, et al. (2010) Phosphorylation of Exo1 modulates homologous recombination repair of DNA double-strand breaks. *Nucleic Acids Res* 38:1821–1831.
- Makharashvili N, et al. (2014) Catalytic and noncatalytic roles of the CtIP endonuclease in double-strand break end resection. *Mol Cell* 54:1022–1033.
- Ziv Y, et al. (2006) Chromatin relaxation in response to DNA double-strand breaks is modulated by a novel ATM- and KAP-1 dependent pathway. *Nat Cell Biol* 8:870–876.
- Helmkink BA, et al. (2011) H2AX prevents CtIP-mediated DNA end resection and aberrant repair in G1-phase lymphocytes. *Nature* 469:245–249.
- Tubbs AT, et al. (2014) KAP-1 promotes resection of broken DNA ends not protected by γ -H2AX and 53BP1 in G₁-phase lymphocytes. *Mol Cell Biol* 34:2811–2821.
- Bothmer A, et al. (2010) 53BP1 regulates DNA resection and the choice between classical and alternative end joining during class switch recombination. *J Exp Med* 207:855–865.
- Yamane A, et al. (2013) RPA accumulation during class switch recombination represents 5'-3' DNA-end resection during the S-G2/M phase of the cell cycle. *Cell Reports* 3:138–147.
- Cortez D, Wang Y, Qin J, Elledge SJ (1999) Requirement of ATM-dependent phosphorylation of brca1 in the DNA damage response to double-strand breaks. *Science* 286:1162–1166.
- Jaspers JE, et al. (2013) Loss of 53BP1 causes PARP inhibitor resistance in Brca1-mutated mouse mammary tumors. *Cancer Discov* 3:68–81.
- Johnson N, et al. (2013) Stabilization of mutant BRCA1 protein confers PARP inhibitor and platinum resistance. *Proc Natl Acad Sci USA* 110:17041–17046.
- Xu G, et al. (2015) REV7 counteracts DNA double-strand break resection and affects PARP inhibition. *Nature* 521:541–544.
- Tkáč J, et al. (2016) HELB is a feedback inhibitor of DNA end resection. *Mol Cell* 61:405–418.